# INVERSE SIMULATION USING DIFFERENTIATION AND INTEGRATION-BASED APPROACH APPLIED TO THE PENDULUM WITH SPRING MODEL

**Euler Gonçalves Barbosa, euleregb@iae.cta.br**
CTA/IAE – Instituto de Aeronáutica e Espaço
Praça Marechal Eduardo Gomes, 50, CEP 12.228-904
São José dos Campos – SP

**Waldemar de Castro Leite Filho, waldemarwclf@iae.cta.br**
CTA/IAE – Instituto de Aeronáutica e Espaço
Praça Marechal Eduardo Gomes, 50, CEP 12.228-904
São José dos Campos - SP

**Luiz Carlos Sandoval Góes, goes@ita.br**
ITA - Instituto Tecnológico de Aeronáutica
Praça Marechal Eduardo Gomes, 50, CEP 12.228-904
São José dos Campos - SP

***Abstract.*** *This paper presents an analysis of inverse simulation applied to a nonlinear system using differentiation and integration-based approaches. The nonliner system consists of a pendulum with spring and a mass tip attached at the end. The equations of motion have nonlinear terms coupling two degrees of freedom, and can represent several linear and nonlinear systems widely considered in control system analysis. The inverse simulation using differentiation and integration-based approach is applied in order to find the input time histories necessary to impose the mass tip to follow a predetermined path and consequentily, is possible to define requirements of force, torque, angular and linear velocities due to the actuator. The results from simulations are presented, showing advantages and disvantages according to the method, as well as analysis of influences due to linearization processes, Newton-Raphson algorithm and model simplifications. It can be observed oscillations through the signals using inverse simulation technique with the traditional methods based on the Newton-Raphson algorithm, and so, aspects concerning to controlability and observability theory are discussed. These aspects are of great interest for applications in closed-loop system design.*

***Keywords:*** *Inverse Simulation, Modeling, Nonlinear systems*

## 1. INTRODUCTION

The conventional simulation technique determines the output response of a model for a set of known inputs and initial conditions. All simulations models are so-called input-output models, that is, they yield the output of the system given the input to its interaction subsystems. The inverse simulation, at other hand, is intended to determine a corresponding input time history that can yield a prescribed output. There are many techniques to solve the inverse simulation, e. g., the differentiation and integration approaches that are discussed in this work. Oscillations appear around the nominal solution depending the choice of method and sample rate, so in this way is presented the results obtained from analysis of inverse simulation based on differentiation and integration approach using the well-known pendulum with spring model. The analysis can be extended to other nonlinear models as well as discussing of instabilities from the results.

Consider the second-order linear model representing the RLC electronic circuit or a mass-spring-dashpot mechanical system shown in Fig. 1.1.(a) and (b). In many applications, mechanicals actuators or power generators are chosen using inverse simulation, where the mass should follow a prescribed path, or the output voltage across the capacitor is known.
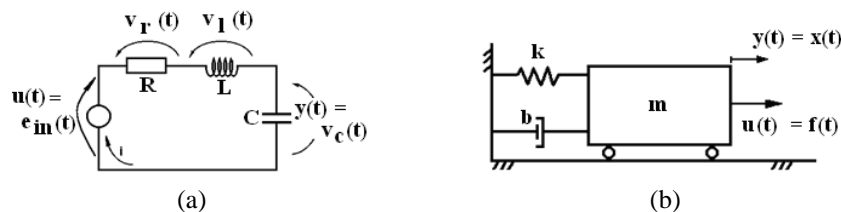


Figure 1.1. (a) RLC and (b) mass-spring-dashpot models.

The forward simulation, represented in Figure 1.2(a), obtain the output time history across the capacitor voltage $v_c(t)$ or mass position $x(t)$, due to known input (input voltage $e_{in}(t)$ or force on mass $f(t)$) and known model. The linear identification process, represented in Fig. 1.2(b), consider the input - output time histories from real or simulated data and by means of an algorithm, linear or nonlinear model can be obtained.

(a) Forward Simulation          (b) Identification process          (c) Inverse Simulation
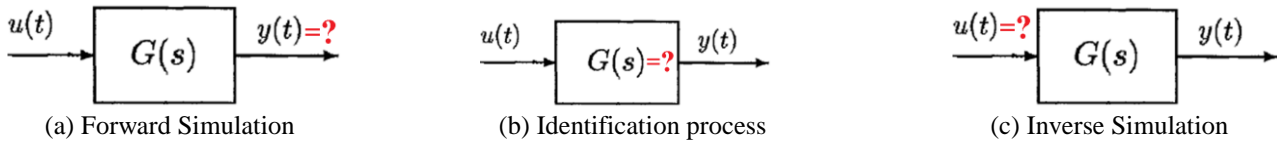
Figure 1.2. Dynamic Systems Simulation and Identification.

The Dynamic System Simulation takes some input signals of special interest and commonly used in system analysis. The step functions, ramp functions (or sawtooth signal), accelerations functions, impulse functions and sinusoidal functions are the signals to the input *u(t)*. Using the Inverse Simulations technique, it can be accessed the analysis in frequency-domain, transient-response (overshoot, delay time, rise time and peak time), as well as position and velocity gains can be accessed in this analysis, defining limits (current, power, torque, force and voltage) and requirements for control system designs. The sections as follow present results obtained from forward and inverse simulations applied to the pendulum with spring model using differentiation and integral-based approach using the inputs mentioned.

## 2. INVERSE SIMULATION

### 2.1. Differentiation-Based Approach

The Inverse Simulation with differentiation-based approach (SIAD) can be applied to the nonlinear state equations and the output equations. Let the initial value problem, described by the nonlinear system,

$$\dot{x} = f(x, u) \qquad\qquad x(0) = x_0 \tag{2.1}$$

where $x$ is the state vector, $u$ is the control vector and $y$ the output vector. The $x(0) = x_0$ is a given set of initial conditions and completes the problem. The output equation is

$$y = g(x) \tag{2.2}$$

differentiating Eq. 2.2 with respect to $x$, become

$$\dot{y} = \frac{dg}{dx} d\dot{x} = \frac{dg}{dx} f(x, u) \tag{2.3}$$

Assuming that Eq. (2.3) is invertible with respect to $u$, so we can explicit $u$ as follows

$$u = h(x, \dot{y}) \tag{2.3}$$

that inserted in Eq. (2.1), results in

$$\dot{x} = f(x, h(x, \dot{y})) = F(x, \dot{y}) \tag{2.4}$$

The differentiation-based approach defines the following equations to the derivatives, nonlinear state equations and output equation

$$F_1(x_n, u_n) = f(x_n, u_n) - \frac{x_n - x_{n-1}}{\Delta t} \tag{2.5}$$

$$F_2(x_n, u_n) = g(x_n) - y_n \tag{2.6}$$

These new functions are inserted in the Newton-Raphson method, in such way that is desired to reach predefined values close to zero. The corresponding values of $x_n$ and $u_n$ are then the required quantities. In other words, these new functions should tends to zero under predefined limits of precision and ($x_n$ , $u_n$) are the corresponding roots.

The Newton-Raphson method used in this work consists of the following equations for linear or nonlinear equations (Murray-Smith 2000).

$$\begin{bmatrix} (x_n)_m \\ (u_n)_m \end{bmatrix} = \begin{bmatrix} (x_n)_{m-1} \\ (u_n)_{m-1} \end{bmatrix} - \begin{bmatrix} \dfrac{\partial F_1}{\partial x} & \dfrac{\partial F_1}{\partial x} \\ \dfrac{\partial F_2}{\partial x} & \dfrac{\partial F_1}{\partial x} \end{bmatrix}^{-1} \begin{bmatrix} F_1\big((x_n)_{m-1},(u_n)_{m-1}\big) \\ F_2\big((x_n)_{m-1},(u_n)_{m-1}\big) \end{bmatrix} \tag{2.7}$$

The vector time history contains the states and input, obtained simultaneously during the iterative process. The matrix of partial derivatives is the well-known Jacobian $J$.

## 2.2. Integration-Based Approach

Hess et al. proposed a method based on numerical integration for the inverse simulation, named here SIAI, and involves iterative procedures. The nonlinear equations described by Eq. (2.1) are discretized as follow, where input is assumed constant during the discretization interval *T*. Newton's method is used to correct the initial guess of the input based on the Jacobian and errors. So, in this way, become

$$(\dot{x}_{n-1})_m = f\big[(x_{n-1})_m,(u_{n-1})_m\big] \tag{2.8}$$

Integrating the energy variables to obtain the states as

$$(x_n)_m = \int_{t_{n-1}}^{t_n} (\dot{x}_{n-1})_m \, dt + (x_{n-1})_m \tag{2.9}$$

the output *y* written as

$$(y_n)_m = g\big[(x_n)_m\big] \tag{2.10}$$

and defining the error function $e_n$ as

$$(e_n)_m = (y_n)_m - \bar{y}_n \tag{2.11}$$

initially the error function calculates the difference between the estimative of output and the desired value. If this difference is grather than a pre-established limit, so the Newton-Raphson algorithm is applied to obtain new values to the input, as follow

$$(u_{n-1})_{m+1} = (u_{n-1})_m - [J]^{-1}(e_n)_m. \tag{2.12}$$

This iterative process continues with m being incremented until all errors in Eq (2.11) were under threshold limits.

## 3. PENDULUM WITH SPRING INVERSE SIMULATIONS

### 3.1. Mathematical model

The Figure 3.1 shows the pendulum with spring and a mass tip attached at the end. There is no damping and the variables $r$ and $\theta$ are the two degrees of freedom. The spring is linear and L is its initial length.
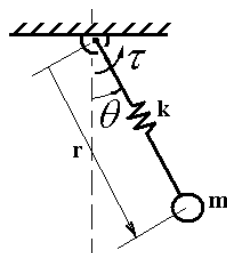


Fig. 3.1 – Pendulum with spring

The nonlinear equations of motion are

$$\begin{cases} \ddot{r} - r\dot{\theta}^2 - g\cos\theta + \dfrac{k}{m}(r - L) = 0 \\ r\ddot{\theta} + 2\dot{r}\dot{\theta} + g\sin\theta = \tau \end{cases} \tag{3.1}$$

with the input torque

$$\tau = A\sin(2\pi f_0 t) \tag{3.2}$$

The output equation is

$$y(t) = \theta \tag{3.3}$$

Defining the state and energy variables

$$\underline{x} = \begin{bmatrix} x_1 & x_2 & x_3 & x_4 \end{bmatrix}^T \tag{3.4}$$

$$\underline{x} = \begin{bmatrix} r & \dot{r} & \theta & \dot{\theta} \end{bmatrix}^T \tag{3.5}$$

$$\underline{\dot{x}} = \begin{bmatrix} \dot{x}_1 & \dot{x}_2 & \dot{x}_3 & \dot{x}_4 \end{bmatrix}^T \tag{3.6}$$

$$\underline{\dot{x}} = \begin{bmatrix} \dot{r} & \ddot{r} & \dot{\theta} & \ddot{\theta} \end{bmatrix}^T \tag{3.7}$$

so the state equations become

$$\begin{cases} \dot{x}_1 = x_2 \\ \dot{x}_2 = x_1 x_4^2 + g\cos x_3 - \dfrac{k}{m}x_1 + \dfrac{k}{m}L \\ \dot{x}_3 = x_4 \\ \dot{x}_4 = -2\dfrac{x_2}{x_1}x_4 - \dfrac{g}{x_1}\sin x_3 + \dfrac{u}{x_1} \end{cases} \tag{3.8}$$

and the output equation

$$y(t) = \theta \tag{3.9}$$

This completes the nonlinear mathematical model to the pendulum.

## 3.2. Inverse Simulation using differentiation-based approach

This approach requires the use of Eq. (2.1). First of all, isolating the radial and angular accelerations, become

$$\begin{cases} \ddot{r} = r\dot{\theta}^2 + g\cos\theta - \dfrac{k}{m}r + \dfrac{k}{m}L \\ \ddot{\theta} = -\dfrac{2\dot{r}\dot{\theta}}{r} - \dfrac{g\sin\theta}{r} + \dfrac{\tau}{r} \end{cases} \tag{3.10}$$

so the state and output equations are

$$\begin{cases} \dot{x}_1 = x_2 \\ \dot{x}_2 = x_1 x_4^2 + g\cos x_3 - \dfrac{k}{m}x_1 + \dfrac{k}{m}L \\ \dot{x}_3 = x_4 \\ \dot{x}_4 = -2\dfrac{x_2}{x_1}x_4 - \dfrac{g}{x_1}\sin x_3 + \dfrac{u}{x_1} \\ y = \theta = x_3 \end{cases} \tag{3.11}$$

Approximating the derivative term as

$$\dot{x}_1 \cong \frac{x_1^n - x_1^{n-1}}{T} \quad \text{and} \quad \dot{x}_2 \cong \frac{x_2^n - x_2^{n-1}}{T} \tag{3.12}$$

$$\dot{x}_3 \cong \frac{x_3^n - x_3^{n-1}}{T} \quad \text{and} \quad \dot{x}_4 \cong \frac{x_4^n - x_4^{n-1}}{T} . \tag{3.13}$$

The forward simulation was realized using simulink from Matlab and the model (3.1) is presented in Fig. 3.2 (left).
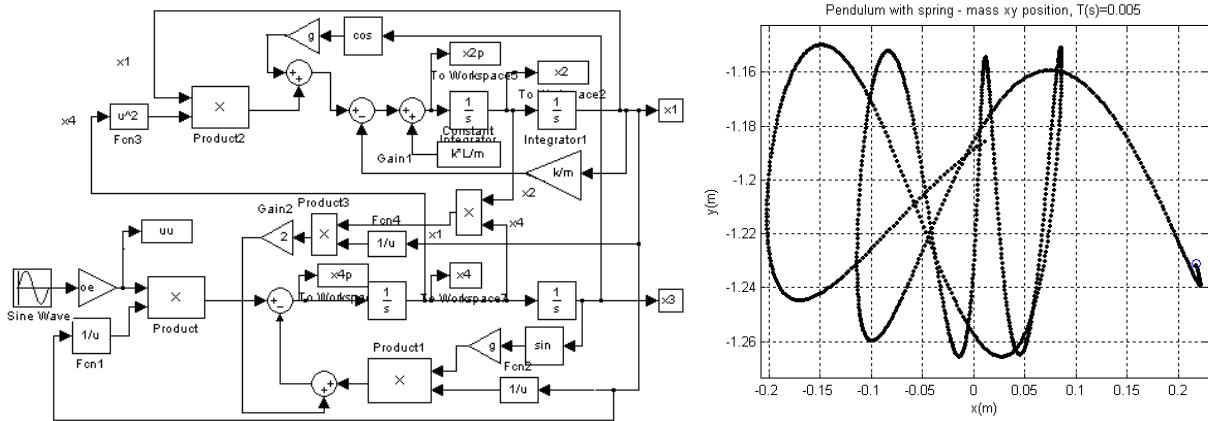


Figure 3.2. (left) Pendulum with spring forward simulations and (right) *xy* mass position for sinusoidal torque input

The Figure (3.2 left and right) shows the results from forward simulation and the Table 1 shows the simulation parameters. The results from forward simulations are shown in Fig. (3.3-rigth) and the complete data set are compiled in Fig. 3.4. The path followed by the mass can be observed, as well as the initial values (a circle plotted) for $r$ and $\theta$. The results from forward and inverse simulations for a sinusoidal input are presented in Fig (3.2-right). It can be observed in Fig (3.3 - left) the data from inverse simulation using T=10 ms and oscillation in 0.5 s. The Fig. (3.3-right) shows the states time histories from forward and inverse simulations.

The Figure (3.4) shows the results with the same parameters, but with sample period ten times lower (T=0.005). The oscillations in 0.5s are lower and the input is obtained with good precision. The Figure 3.5 shows simulations with different values to the sample period.

Table 1. Simulation parameters

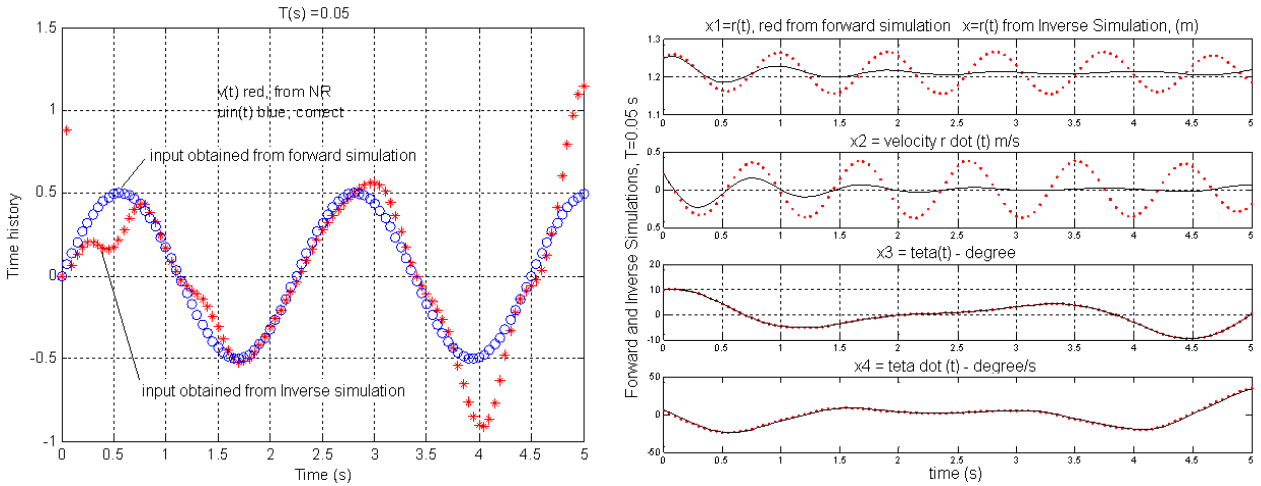| Parameter | Value |
|---|---|
| Start time, $t_{start}$ (s) | 0.0 |
| Finish time, $t_{end}$ (s) | 5.0 |
| Mass, $m$ (kg) | 0.3 |
| Spring constant, k (N/m) | 14.0 |
| Length, L(m) | 1.0 |
| Sample Period, T (s) | 0.05 |
| gravity, g (m/s) | 9.81 |
| Amplitude torque, T (Nm) | 0.5 |
| Frequency excitation, f (Hz) | 1/ 2.25 |
| $x_1(0) = r(0)$, (m) | 1.25 |
| $\dot{x}_1(0) = \dot{r}(0)$, (m/s) | 0.2 |
| $x_2(0) = \theta(0)$, (rd) | $10\pi/180$ |
| $\dot{x}_2(0) = \dot{\theta}(0)$, (rd/s) | $5\pi/180$ |

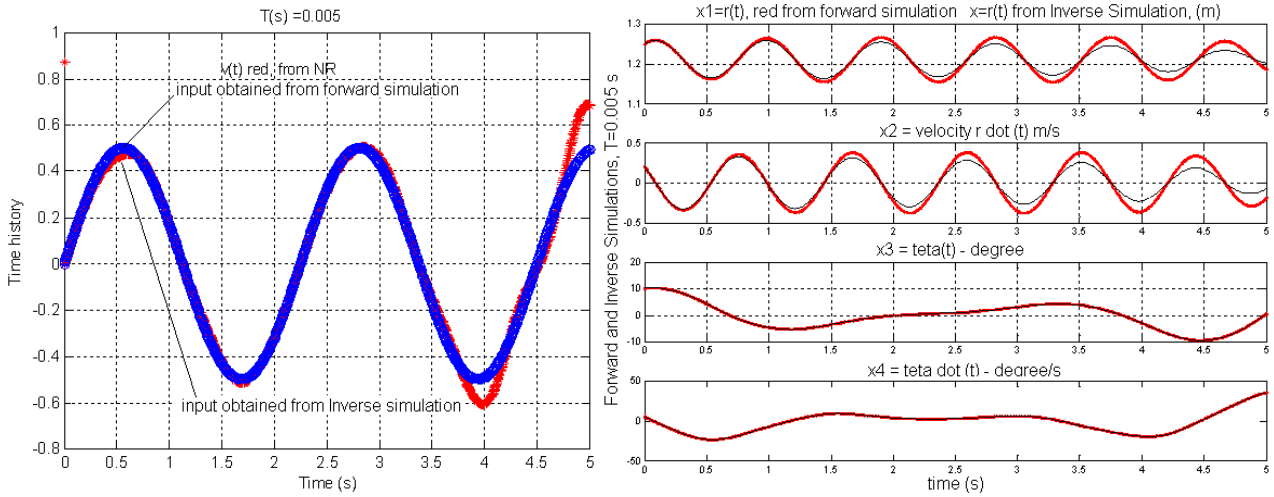Figure 3.3. Results from SIAD Simulation, T = 0.05s (left) input and (right) state variables.



Figure 3.4. Results from SIAD Simulation, T = 0.005s (left) input and (right) state variables.



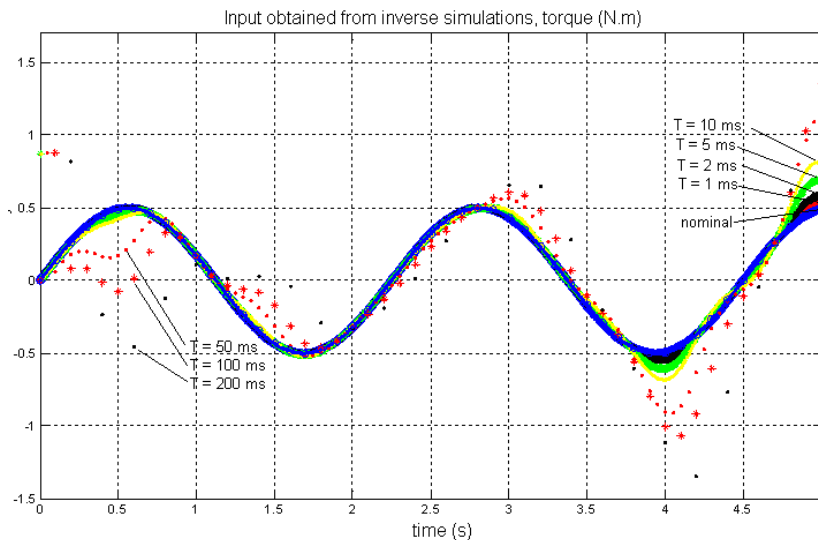Figure 3.5. Results using T=1ms, 2ms, 5ms, 10ms, 50ms, 100ms and 200ms (7 time histories + nominal input)

The Figures (3.6) and (3.7) show the results from inverse simulation SIAD for a unit-step input, using T=10ms and T=1 ms respectively. The Figures (3.8) show the results from inverse simulation SIAD for a sawtooth input, using T=1ms.

Figure 3.6. Results using SIAD - sawtooth input, T = 0.01s: (left) nominal and obtained from ISAD: (rigth) zoom.

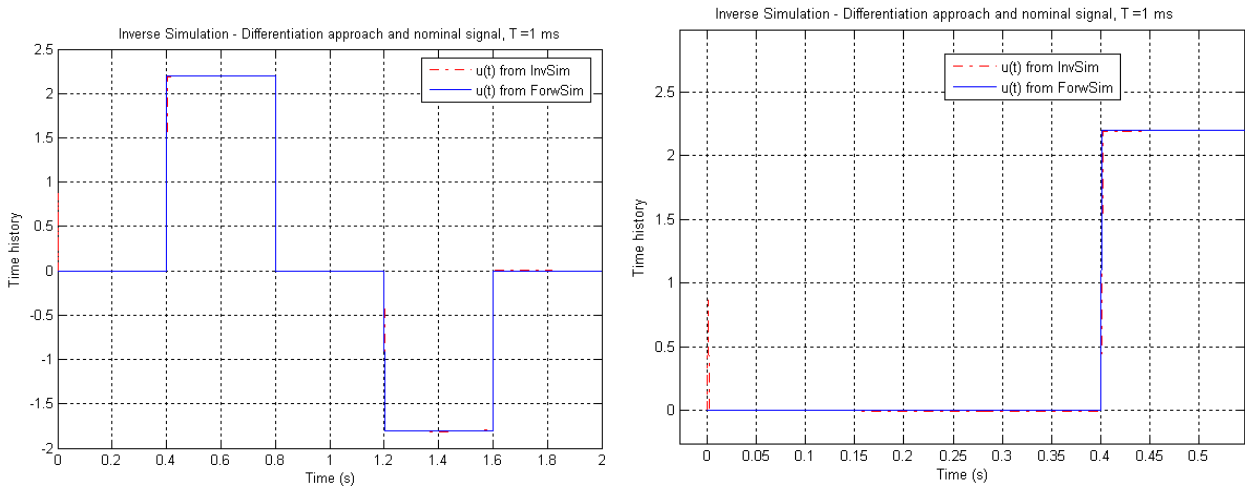

Figure 3.7. Results using SIAD - sawtooth input, T = 0.001s: (left) nominal and obtained from ISAD: (rigth) zoom.
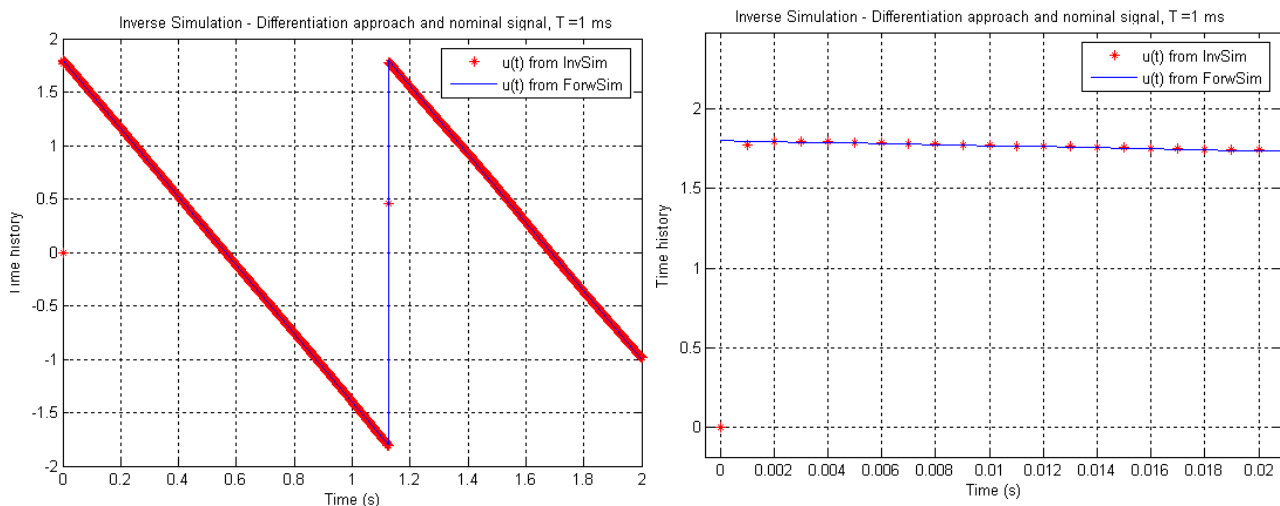


Figure 3.8. Sawtooth input, T = 0.001s: (a) nominal and obtained from ISAD: (b) Zoom.

## 3.3. Inverse Simulation using integration-based approach

This approach requires the discretized state equation in the form of Eq. (2.8). So we obtain the following equations.

$$
\begin{cases}
\dot{x}_1^n = x_2^n \\[2mm]
\dot{x}_2^n = x_1^n \left( x_4^n \right)^2 + g \cos x_3^n - \dfrac{k}{m} x_1^n + \dfrac{k}{m} L \\[2mm]
\dot{x}_3^n = x_4^n \\[2mm]
\dot{x}_4^n = -2 \dfrac{x_2^n}{x_1^n} x_4^n - \dfrac{g}{x_1^n} \sin x_3^n + \dfrac{u^n}{x_1^n}
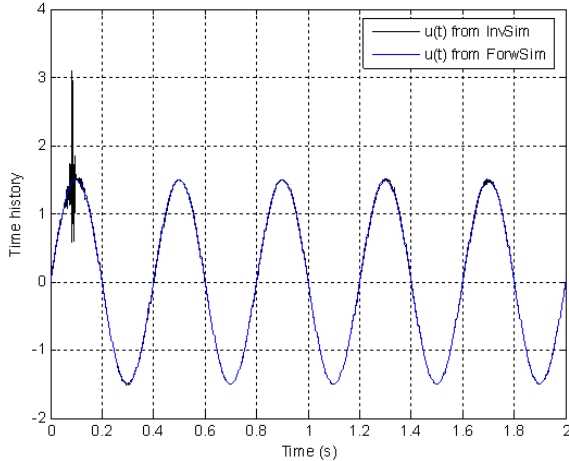\end{cases}
\tag{3.14}
$$

and approximating the integration process as

$$
x_{t_{k+1}} = \int_{t_k}^{t_{k+1}} \dot{x}(t) dt + x(t_k)
\tag{3.15}
$$

$$
\underline{y}(t_{k+1}) = \underline{x}(t_{k+1})
\tag{3.16}
$$

The results are presented in Figures as follow. The Figure (3.9) shows the results for a sinusoidal input, Fig (3.10) for a step input and Fig (3.11) for a sawtooth input signal. All of them using T=1ms of sample period. It can be observed oscillations due to numerical calculations during the Newton-Raphson calculations and the medium of the signal along time $t$ gives the final input. The nominal torque-input was obtained on all cases.
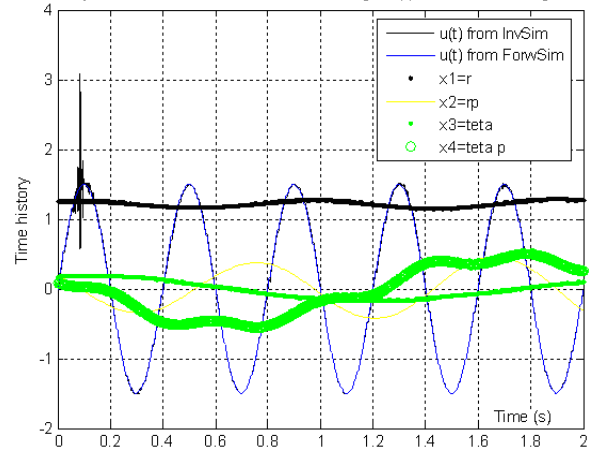


Figure 3.9. Sinusoidal torque input – Results from inverse simulations using integral approach – T=1ms (left) only input and (rigth) input and states x1, x2, x3, x4.
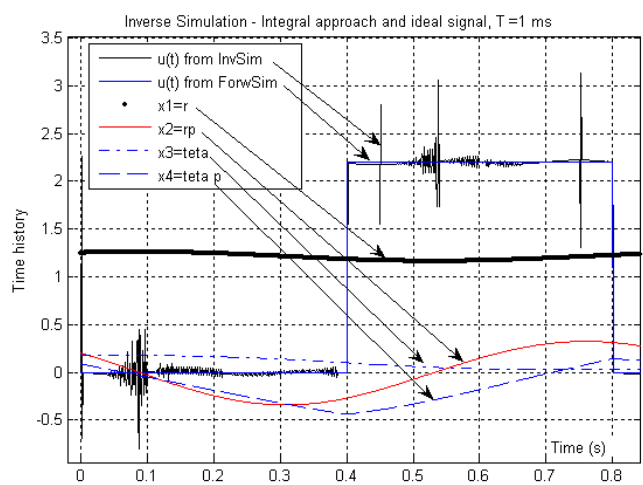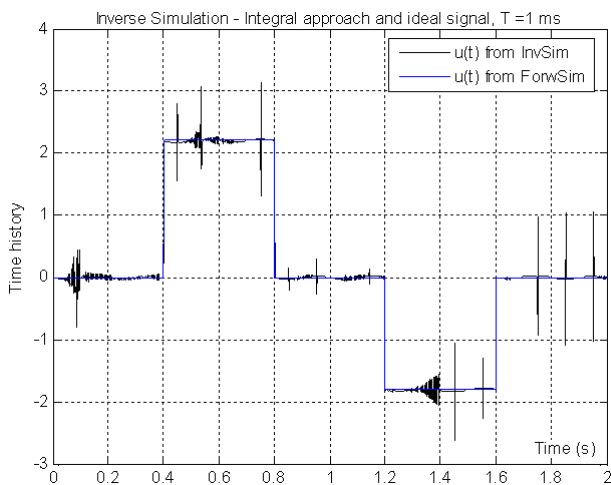


Figure 3.10. Step torque input – Results from inverse simulations using integral approach – T=1ms (left) only input and (rigth) input and states x1, x2, x3, x4.
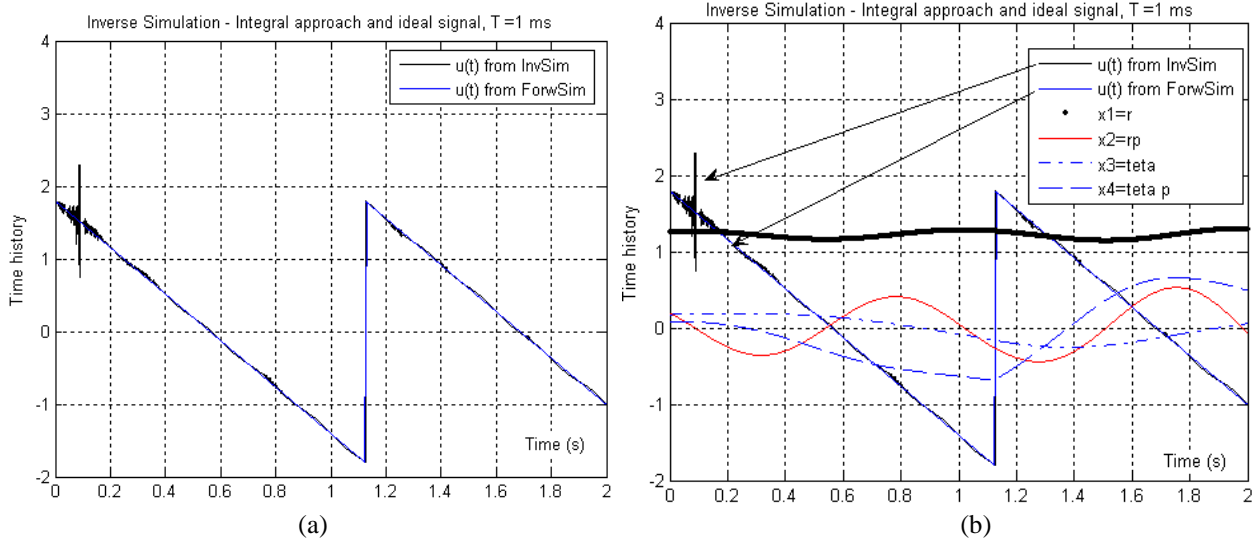
Figure 3.11. Sawtooth torque input – Results from inverse simulations using integral approach – T=1ms
(left) only input and (rigth) input and states x1, x2, x3, x4.

### 1.3. Differentiation and integration-based approach Comparison

The figures as follow present the results obtained from inverse simulation using differentiation approach (Fig. 3.12. left) and using integration approach (Fig 3.12. right).
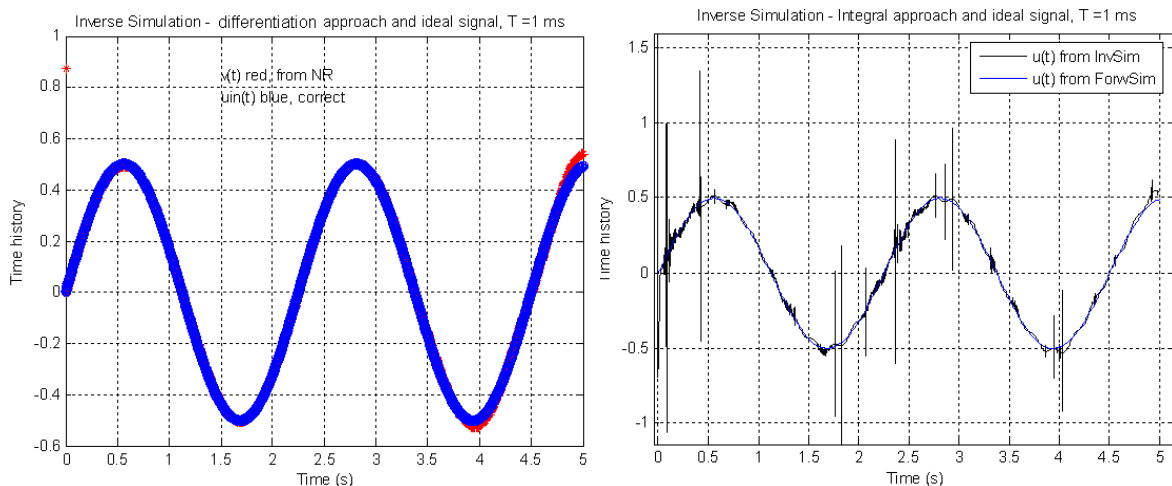


Figure 3.12. Comparison: (left) using differentiation approach and (rigth) using integration approach

It is observed that, using SIAD, the first point for input has incorrect value and the Newton-Raphson produces many iterations leading to greater total time of simulation. The SIAI method produces results with oscillation where the medium is correct (Fig. 3.12. right), the total time of simulation is relative fast and the Newton-Raphson algorithm has shown few iterations for convergence.

### 7. RECOMMENDATIONS

The SIAD approach performs the calculation of discrete derivatives and if noise is present, it is necessary the presence of a filter to obtain better results. At other hand, the application of Inverse Simulations requires the desired output, and so, it can be used data directly from mathematical functions or sampled data from functions. In the pendulum with spring, the linear and angular position are defined easily from functions and/or charts. The SIAI approach can take the presence of noise and produces better results than SIAD.

The first value obtained from SIAD can assume better result if the state values are available, and in these cases it is possible to set the initial values in the algorithm. The application of inverse simulation in nonlinear system leads to desired input signal, not mattering if the system is stable or unstable.

The symbolic language was used to perform the calculation of partial derivatives to the Jacobian. This tool is very useful for complex systems, where the dynamic is represented by nonlinear equations consisting of combination of trigonometric functions and others. In these cases are dynamics from aircraft equations of motion with Euler's angle or quaternion parameters. The inclusion of others dynamics, like a double pendulum and dumping, are easily implemented in the algorithm, becoming the SIAD and SIAI a powerful tool of analysis.

## 8. CONCLUSIONS

The application of Inverse Simulation techniques using differentiation and integration-based approach on the pendulum with spring model allowed to obtain the torque input time history. The results from both techniques show a good convergence and only the SIAI was performed faster than SIAD. The pendulum with spring model can be extended to many others similar dynamic system, and in this way, the results obtained in this analysis can easily extended for others issues. The typical application of SIAI leads to signals with oscillations and it is necessary a low-pass filter to smooth data, obtaining the desired input.

The main conclusion of this work is that the inverse simulation can be applied to the pendulum with spring in order to access the input necessary to follow a pre-established path. So, obtained the input, the actuators can be specified or a class of actuators can be chosen to perform the control torque to the pendulum.

## 9. ACKNOWLEDGEMENTS

## 10. REFERENCES

Avanzini, G., Matteis, G. 2001, "Two-Timescale Inverse Simulation of a Helicopter Model", Journal Of Guidance, Control, And Dynamics, Vol. 24, No. 2, March–April 2001.

Borri, M., Bottasso, C. L., Montelaghi, F., 1997, "Numerical Approach to Inverse Flight Dynamics", Journal Of Guidance, Control, And Dynamics, Vol. 20, No. 4, July–August 1997.

Cook, A. C., 1986, "*Nonlinear Dynamical Systems*", Prentice-Hall International.

Franklin, G. F.; Powell, J. D.; Emami-Naeini, 1991, "Feedback control of dynamic systems. New York, NY.: Addison Wesley Publishing Company.

Hess, R.A., Gao, C., Wang, S.H., 1991, "Generalized technique for inverse simulation applied to aircraft maneuvers". AIAA Journal of Guidance, Control, and Dynamics; 14(5):920–6.

Lee, S., Kim, Y., 1997, "Time-Domain Finite Element Method for Inverse Problem of Aircraft Maneuvers", Journal Of Guidance, Control, And Dynamics, Vol. 20, No. 1, January–February.

Linghai L., Murray-Smith D.J., Thomson, D. G., 2007, "Sensitivity-Analysis Method for Inverse Simulation Application", Journal ff Guidance, Control, And Dynamics, Vol. 30, No. 1, January–February.

Murray-Smith, D.J., 1998, "*Methods for the external validation of continuous system simulation models: A review*". Elsevier Science, Mathematical and Computer Modelling of Dynamic Systems, Vol. 4, pp. 5-31.

Murray-Smith, D. J., 2000, "*The inverse simulation approach: a focused review of methods and applications*", Mathematics and Computers in Simulation, pp. 239-247.

Murray-Smith, D.J., Linghai Lu , 2007, Inverse Simulation Methods And Applications, Proc. EUROSIM 2007, 9-13, Sept. 2007, Ljubljana, Slovenia.

Sastry, S., 1999, "Nonlinear systems: analysis, stability, and control". New York: Spring-Verlag.

Sibilski, K., Zyluk, A., 2006, An Inverse Simulation Study on Wing Adapter Kit Dynamics and Control in Prescribed Trajectory Flight, 44th AIAA Aerospace Sciences Meeting and Exhibit, 9 - 12 January 2006, Reno, Nevada.

Stoker, J. J., 1992, "*Nonlinear Vibrations – in Mechanical and Electrical Systems*", Interscience Publishers, Inc., New York.

Thomson, D. G., 1998, "*The principles and practical application of helicopter inverse simulation*", Simulatioon Practice and Theory, pp. 47-62.

## 5. RESPONSIBILITY NOTICE

The author is the only responsible for the printed material included in this paper.